

On the Release and Renewal of Freshwater in the Beaufort Gyre of the Arctic Ocean

QIANG WANG¹¹ Alfred Wegener Institute, Helmholtz Centre for Polar and Marine Research, Bremerhaven, Germany


(Manuscript received 5 September 2023, in final form 6 February 2024, accepted 18 March 2024)

ABSTRACT: The Arctic Beaufort Gyre plays a critical role in climate and marine ecosystems. This study investigates the response of the liquid freshwater in the Beaufort Gyre to various wind perturbations using numerical simulations. A new diagnostic called “freshwater renewal” is introduced, which quantifies the amount of freshwater that has entered the Beaufort Gyre since a specific point in time. The findings reveal that the process of freshwater renewal is persistently efficient in the Beaufort Gyre region, occurring irrespective of the gyre’s status. The spatial distribution of freshwater renewal varies, influenced by factors such as wind forcing and gyre circulation patterns. Cyclonic wind perturbation associated with a negative Beaufort high sea level pressure anomaly triggers freshwater release from the Beaufort Gyre, with freshwater export and renewal dependent on wind-perturbation locations and time scales. While some released Beaufort Gyre freshwater exits the Arctic Ocean through the Davis and Fram Straits, a considerable portion could remain within the Arctic Ocean for many years under specific conditions. Wind perturbation associated with the positive Arctic Oscillation enhances the Arctic export of Beaufort Gyre freshwater, mainly through the Fram Strait. The Arctic export of total freshwater and the Arctic export of the portion originating from the Beaufort Gyre have different time scales and magnitudes. Hence, it is essential to collectively examine different freshwater components in order to assess the role of Arctic export in the climate system.

KEYWORDS: Arctic; Ocean dynamics; Freshwater; Gyres

1. Introduction

The Beaufort Gyre is one of the major features of the Arctic Ocean (Figs. 1a,c), which is sustained by the anticyclonic atmospheric circulation associated with the Beaufort high sea level pressure (SLP) (Fig. 1b). It is a large freshwater reservoir, and its freshwater content (FWC) has experienced a considerable increase over the past two decades (McPhee et al. 2009; Proshutinsky et al. 2009; Giles et al. 2012; Morison et al. 2012; Krishfield et al. 2014; Zhang et al. 2016; Q. Wang et al. 2018; Proshutinsky et al. 2019, 2020). The increase primarily occurred during two periods: first from 2004 to 2009, associated with a westward expansion of the gyre (Regan et al. 2019), and second, from 2014 to 2019, associated with an eastward shrinkage of the gyre (Wang and Danilov 2022). These two periods were marked by negative wind curl over the Canada Basin with large magnitude unprecedented within the last six decades (Wang and Danilov 2022). It was quantified that the dramatic decline in Arctic sea ice played a pivotal role in intensifying the accumulation of freshwater within the Beaufort Gyre (Q. Wang et al. 2018). This influence stemmed from two key factors: a reduction in brine rejection and the modification of the circulation pathways of freshwater. Notably, the decline in sea ice contributed to approximately 50% of the freshwater accumulation in the Beaufort Gyre during the 2000s. Recent hydrography observations indicated a slight reduction in the Beaufort Gyre FWC in 2020 and 2021 (Timmermans and Toole 2023).

 Denotes content that is immediately available upon publication as open access.

Corresponding author: Qiang Wang, qiang.wang@awi.de

DOI: 10.1175/JPO-D-23-0184.1

© 2024 American Meteorological Society. This published article is licensed under the terms of the default AMS reuse license. For information regarding reuse of this content and general copyright information, consult the AMS Copyright Policy (www.ametsoc.org/PUBSReuseLicenses).

Arctic freshwater is an important component of the climate system (Serreze et al. 2006; Carmack et al. 2016; Weijer et al. 2022), and the Beaufort Gyre functions as the largest Arctic freshwater reservoir (Proshutinsky et al. 2002, 2015; Timmermans and Toole 2023). Arctic freshwater is exported to the subpolar North Atlantic on both sides of Greenland (Fig. 1a; Rudels 1989; Curry et al. 2014; de Steur et al. 2018; Karpouzoglou et al. 2022), with potential to impact the upper ocean stratification and dense water formation in the subpolar North Atlantic (Aagaard et al. 1985; H. Wang et al. 2018; Weijer et al. 2019; Zhang et al. 2021). Moreover, the Arctic export serves as a conduit for essential nutrients vital to marine ecosystems (Carmack et al. 2016; Azetsu-Scott et al. 2010). Therefore, it is clear that improving our understanding of the dynamical processes associated with the release of freshwater from the Beaufort Gyre is of crucial importance. This importance is underscored by the fact that the Beaufort Gyre currently retains a substantial amount of excess freshwater (Proshutinsky et al. 2019; Wang and Danilov 2022; Lin et al. 2023; Timmermans and Toole 2023).

In this study, we employ model simulations to explore the impact of various wind anomalies on freshwater release from the Beaufort Gyre. We introduce a new diagnostic called “freshwater renewal,” which quantifies the amount of freshwater that has entered the Beaufort Gyre since a specific point in time. We find that even when the Beaufort Gyre is discharging freshwater due to a strong cyclonic wind forcing, the renewal of freshwater in the Beaufort Gyre remains highly effective.

In section 2, we describe the model simulations employed in this study. The main results are provided in section 3, followed by discussion and summaries in sections 4 and 5, respectively.

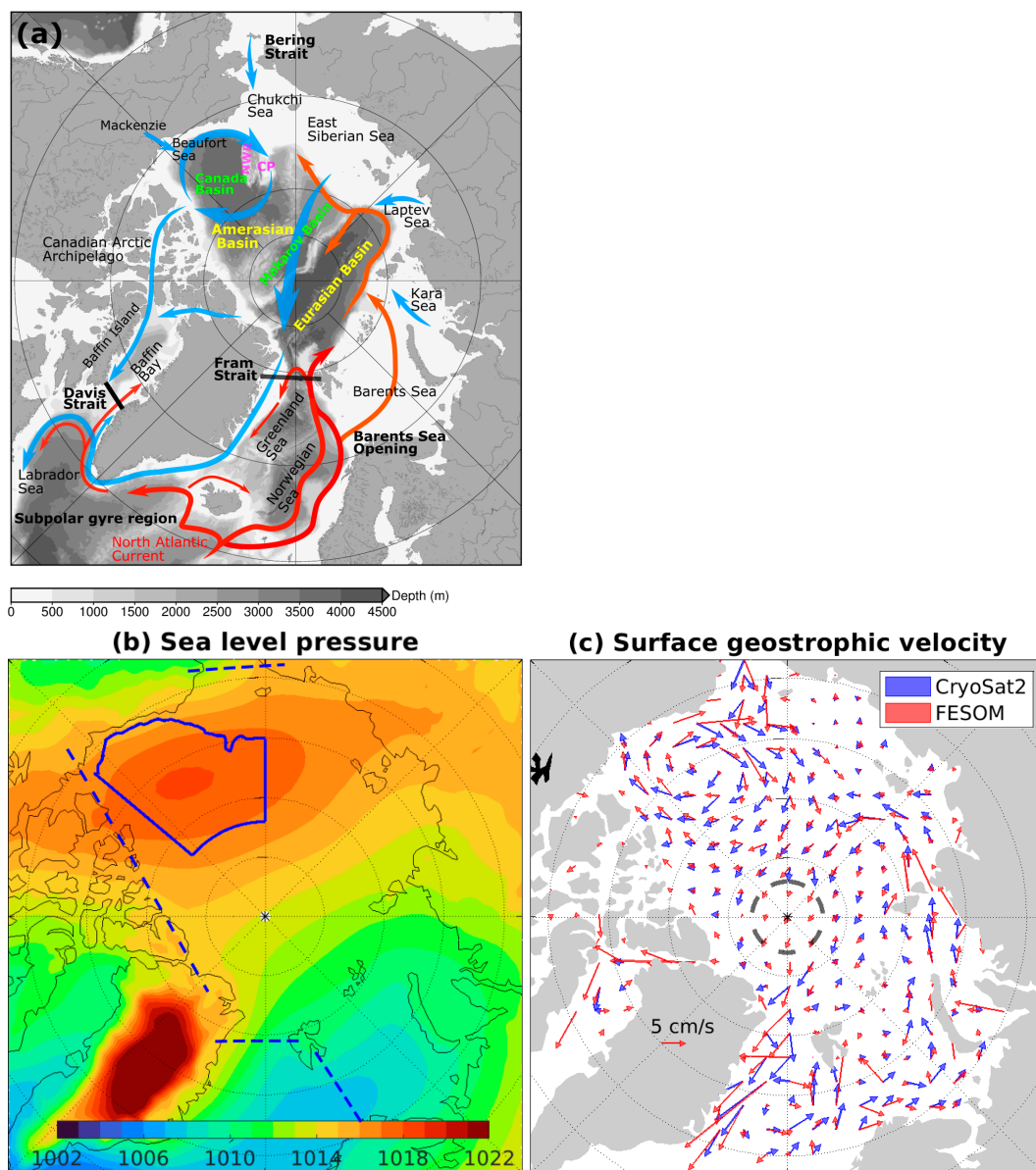


FIG. 1. (a) Schematic of the Arctic Ocean freshwater (blue) and Atlantic water (red) circulation. The background gray color denotes the bottom bathymetry. (b) SLP (hPa) averaged over 1980–2019. (c) Ocean surface geostrophic velocity for 2011–19 estimated from the dynamic ocean topography observed by *CryoSat-2* (Armitage et al. 2017) and simulated in FESOM. In (a), CP stands for Chukchi Plateau and NWR for Northwind Ridge. In (b), the solid blue lines indicate the Beaufort Gyre region defined in this paper, and the dashed blue lines indicate the Arctic Ocean domain used to calculate Arctic FWC.

2. Model configuration and method

In this study, we employed the Finite Element Sea ice Ocean Model (FESOM1.4; Wang et al. 2014; Danilov et al. 2015). It uses unstructured meshes in both its ocean and sea ice components, allowing for variable horizontal resolution. The global configuration utilized here has a horizontal resolution of 4.5 km in the Arctic region and a nominal 1° resolution for most other areas of the globe. Its vertical spacing is 10 m in the upper 100 m and gradually coarsened downward, with a total of 47 z levels.

The simulation was initialized from the Polar Science Center Hydrographic Climatology (PHC3) (Steele et al. 2001) and performed from 1958 to 2021. We used the JRA55-do atmospheric forcing fields and river runoff (Tsujiro et al. 2018). This model configuration has been described and evaluated in previous studies (Q. Wang et al. 2018, 2020; Wang 2021; Wang and Danilov 2022). These studies have shown that the model can reasonably reproduce observed changes in Arctic sea ice and the FWC.

In addition to the aforementioned historical (control) simulation, we conducted a suite of wind-perturbation simulations.

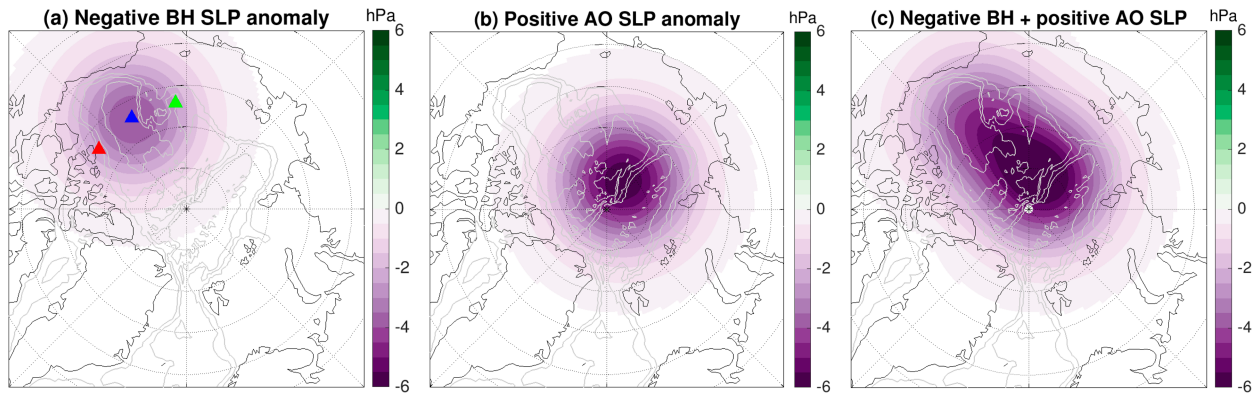


FIG. 2. (a) SLP anomaly of the negative-phase Beaufort high forcing. The plot shows the case with the center of the anomaly located at the center of the Beaufort high climatology, indicated by the blue triangle (used in the BH_center simulation). The green and red triangles denote the center of the SLP anomaly in the BH_west and BH_east cases, respectively. (b) The SLP anomaly of the positive Arctic Oscillation forcing. (c) The SLP anomaly when both the negative Beaufort high forcing (the case with central location) and positive Arctic Oscillation forcing are applied. The wind anomalies corresponding to these SLP anomalies are used in the wind-perturbation experiments.

These simulations closely resemble the control simulation, except that wind anomalies were added to the wind forcing in the calculation of wind stress. The first wind perturbation is the cyclonic wind forcing associated with a negative anomaly of the Beaufort high sea level pressure (Fig. 2a). The center of the wind perturbation aligns with the center of the Beaufort high climatology pattern (Fig. 1b).

In reality, wind anomalies causing the release of freshwater from the Beaufort Gyre region do not always center over the central Canada Basin. To account for such variations, we carried out additional simulations with wind perturbations positioned at different longitudes, either more to the east or to the west (Fig. 2a), while maintaining the same spatial pattern and magnitude. These experiments are labeled BH_center, BH_west, and BH_east, clearly denoting the wind perturbations used (see Table 1). These simulations spanned a duration of 8 years (calendar years 2014–21) starting from the results of the control simulation at the beginning of 2014.

The Arctic Oscillation (Thompson and Wallace 1998) can exert a considerable influence on the accumulation and export of Arctic freshwater (Maslowski et al. 2000; Zhang et al. 2003; Steele et al. 2004; Lique et al. 2009; Condrón et al. 2009; Aksenov et al. 2010; Jahn et al. 2010; Cornish et al. 2020; Morison et al. 2021). During its positive phase, there is a tendency for Arctic freshwater to be exported from the central Arctic to the North Atlantic. Figure 2b shows a wind-perturbation pattern

resembling the positive Arctic Oscillation anomaly. In the experiment named BH_center+AOp, we initialized the simulation using the results from the third year of the BH_center experiment and continued it for 5 years (covering the calendar years 2017–21). This simulation incorporated both the wind perturbations of the negative Beaufort high anomaly at the central location and the positive Arctic Oscillation perturbation. The combined wind perturbation used in this experiment is depicted in Fig. 2c.

To illustrate the impact of downstream conditions in the subpolar North Atlantic on the export of Beaufort Gyre freshwater from the Arctic Ocean, we conducted an additional simulation referred to as BH_center+SPG. In this simulation, we initiated from the results of the third year of the BH_center experiment and ran the model for 3 years (covering the calendar years 2017–19). During these 3 years, we replaced the atmospheric forcing data outside the Arctic Ocean with data from 2014 to 2016. In 2014–16, there was a notable drop in the dynamical sea level in the subpolar gyre, resulting in enhanced freshwater export through the Davis Strait during that period (Wang et al. 2022). In BH_center+SPG, we aimed to reproduce the low sea level condition of 2014–16 for 2017–19. This simulation was carried out with the intention of understanding how the export of freshwater originally located within the Beaufort Gyre can be influenced by the ocean conditions in the subpolar North Atlantic.

TABLE 1. List of experiments.

Name	Forcing perturbation	Period
control		1958–2021
BH_center	Negative Beaufort high anomaly, center	2014–21
BH_west	Negative Beaufort high anomaly, west	2014–21
BH_east	Negative Beaufort high anomaly, east	2014–21
BH_center+AOp	Negative Beaufort high anomaly, center; positive Arctic Oscillation anomaly	2017–21
BH_center+SPG	Negative Beaufort high anomaly, center; forcing outside Arctic replaced	2017–19
BHp	Positive Beaufort high anomaly, center	2014–21

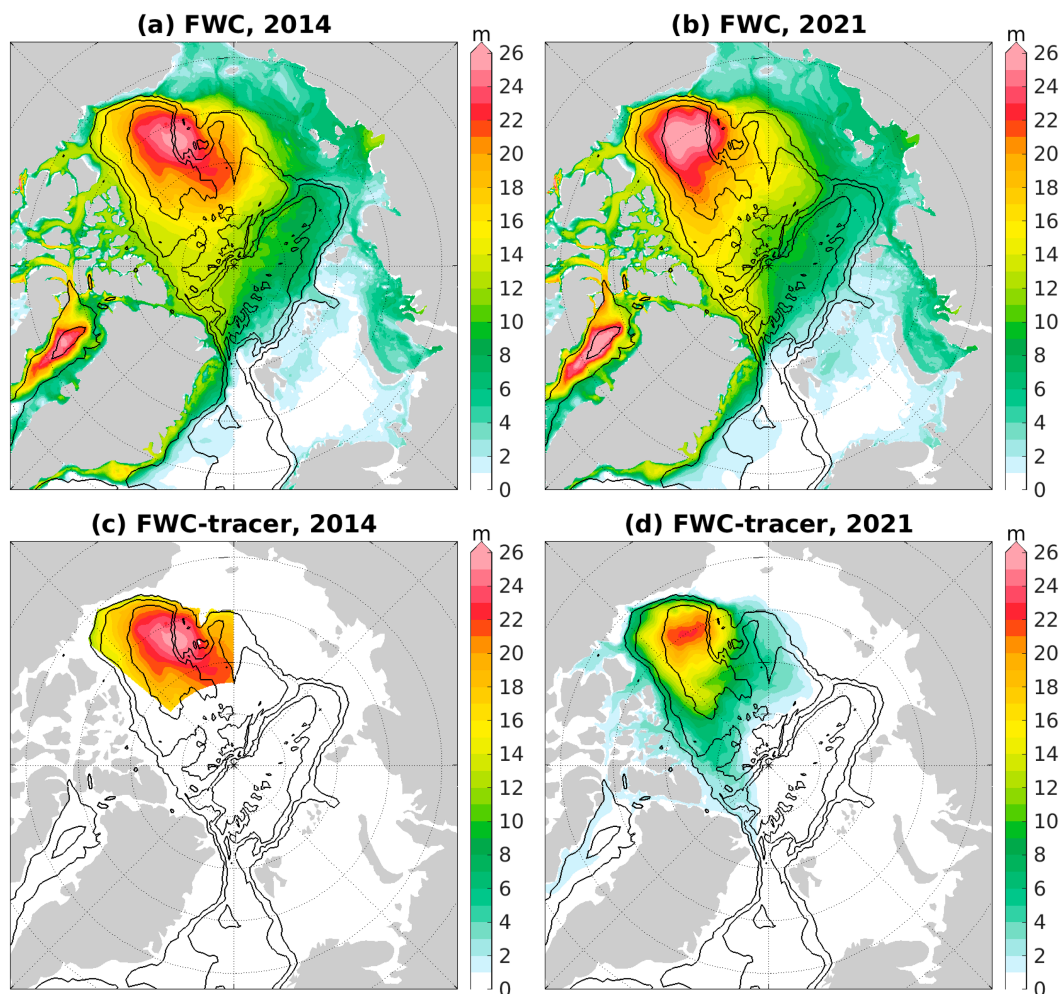


FIG. 3. (a) FWC (m) at the beginning of 2014. (b) FWC in 2021. (c) The initial FWC-tracer content (m), which was set to be equal to the FWC inside the Beaufort Gyre region. (d) The FWC-tracer content in 2021.

The last wind-perturbation experiment, called BHp, is the same as BH_center, but the applied wind perturbation is anticyclonic, with directions opposite to those in BH_center. Different from all other wind-perturbation experiments, BHp represents a scenario of freshwater accumulation in the Beaufort Gyre. With this additional experiment, we will be able to compare the process of Beaufort Gyre freshwater renewal between the scenarios of freshwater release and accumulation.

In line with prior research, we define a vertically integrated FWC within a water column as follows:

$$\text{FWC} = \int_D^0 (S_{\text{ref}} - S)/S_{\text{ref}} dz, \quad (1)$$

where S represents the salinity, S_{ref} is the reference salinity, which is set to the mean salinity of the Arctic Ocean (34.8), and D signifies the depth of the 34.8 isohaline. By integrating the vertically integrated FWC over a specific area, one can obtain the volumetric FWC.

To track the freshwater originally located within the Beaufort Gyre, a passive tracer was introduced in our model simulations. Specifically, at each model grid point located above the 34.8 isohaline within the Beaufort Gyre at the beginning of 2014, we assigned the value $c = (S_{\text{ref}} - S)/S_{\text{ref}}$ to this passive trace; otherwise, it was set to zero. Essentially, at the beginning of 2014, this passive tracer precisely represents the quantitative measure of the FWC present within the Beaufort Gyre. By employing this FWC-tracer, one objective is to discern how the specific freshwater initially situated within the Beaufort Gyre is affected by imposed wind perturbations. The difference between the FWC and the amount of the FWC-tracer in the Beaufort Gyre represents the renewed freshwater in the gyre since the start of the simulations.

3. Results

a. Control simulation

In comparison with 2014, more freshwater is concentrated in the central Canada Basin in 2021 (Figs. 3a,b). The reduction in the FWC across the Chukchi Abyssal Plain and Chukchi Plateau

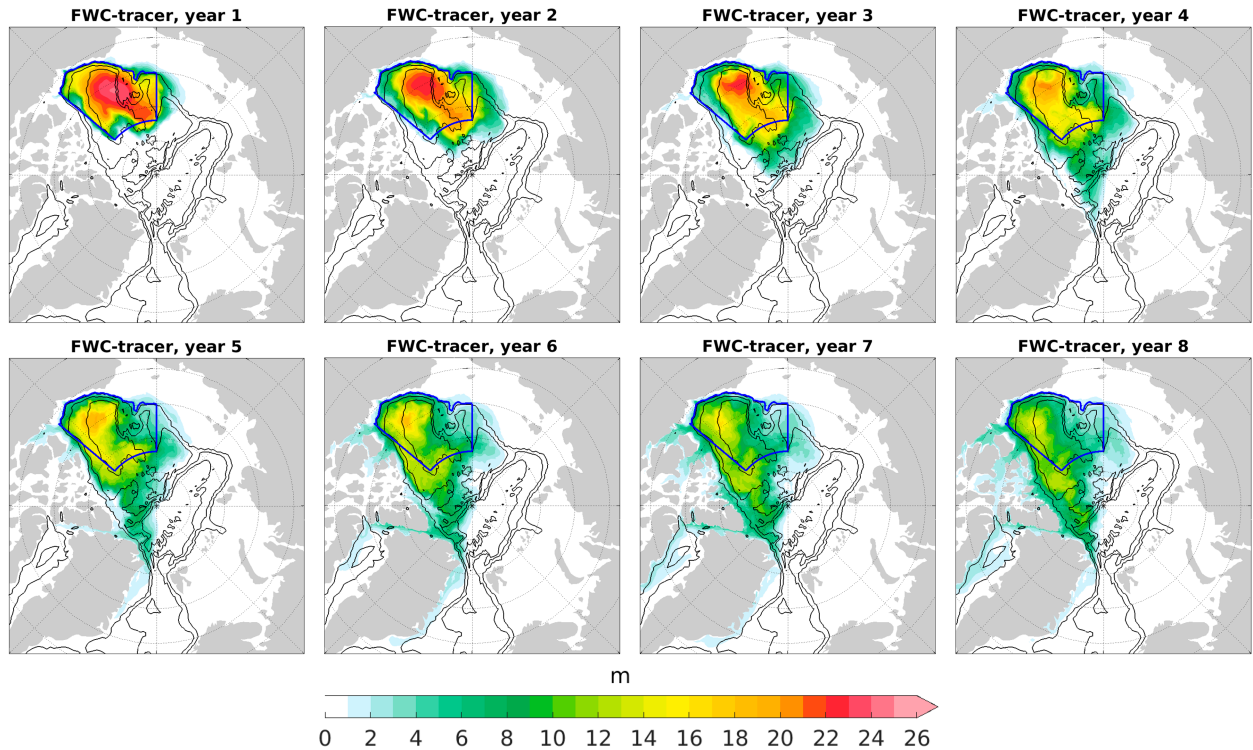


FIG. 4. The annual-mean FWC-tracer content (m) in the simulation BH_center in different model years. The sequence of plots illustrates the evolution of the freshwater originally located in the Beaufort Gyre region under the forcing of cyclonic wind anomalies. The SLP associated with this wind forcing is depicted in Fig. 2a.

in this period reflects the eastward contraction of the Beaufort Gyre, consistent with previous model results and satellite observations (Wang and Danilov 2022; Lin et al. 2023).

Figure 3c presents the distribution of the FWC-tracer at the beginning of 2014, which, as per our definition, mirrors the FWC at that specific time as shown in Fig. 3a. By 2021, a proportion of the FWC-tracer has been released from the Beaufort Gyre, dispersed within the broader Arctic Ocean beyond the Beaufort Gyre region, or exported through the Arctic gateways (Fig. 3d). The reduction in the FWC-tracer content across the Chukchi Abyssal Plain and Chukchi Plateau in this period is consistent with the reduction in the FWC in these regions (Figs. 3b,d). However, the reduction in the FWC-tracer content clearly exceeds the reduction in the FWC. In the central Canada Basin, where the FWC increased in this period, the FWC-tracer content rather decreased (Figs. 3b,d). The above facts suggest that the renewal of freshwater in the Beaufort Gyre region is a general process, irrespective of the gyre's status, whether it is accumulating or releasing freshwater. In the following, we will explore whether and how different wind perturbations can influence the renewal process.

b. Freshwater release from the Beaufort Gyre

The sequence of the FWC-tracer in different model years in the BH_center experiment is shown in Fig. 4. The FWC-tracer is released from the Beaufort Gyre region through both of its northern and western boundaries during the first few years and

mainly through its northern boundary during the last few years. With time, the FWC-tracer remaining in the Beaufort Gyre region becomes mainly confined to the eastern Canada Basin, and the released FWC-tracer shifts closer to the Canadian Arctic Archipelago and Greenland. It takes about 4 years for the FWC-tracer to reach the Fram Strait and about 5 years to reach the Baffin Bay in this experiment (judged with FWC-tracer content of being at least 1 m in Fig. 4). As shown in section 3d, these time scales can be influenced by the applied wind forcing.

The FWC-tracer remaining in the Beaufort Gyre region is noticeably less in the BH_center experiment than in the control simulation (cf. Figs. 5a and 3d). The difference in the FWC-tracer between the two simulations, caused by the cyclonic Beaufort high wind perturbation, is predominantly centered over the southern-central Canada Basin (Fig. 5b). The FWC-tracer that is additionally released by the applied wind perturbation gets accumulated to the north of the Canadian Arctic Archipelago and Greenland, with subsequent export occurring on both sides of Greenland. The pattern of the changes in the FWC induced by the applied wind perturbation differs, exhibiting a negative anomaly in the Canada Basin and a positive anomaly in the Eurasian Basin (Fig. 5c). Examining the time series of changes in the FWC-tracer and FWC within the Beaufort Gyre region, it becomes evident that they initially decrease at different rates. However, their overall reduction within the Beaufort Gyre is found to be similar by the end of the simulations, as indicated by the blue lines in Fig. 6a.

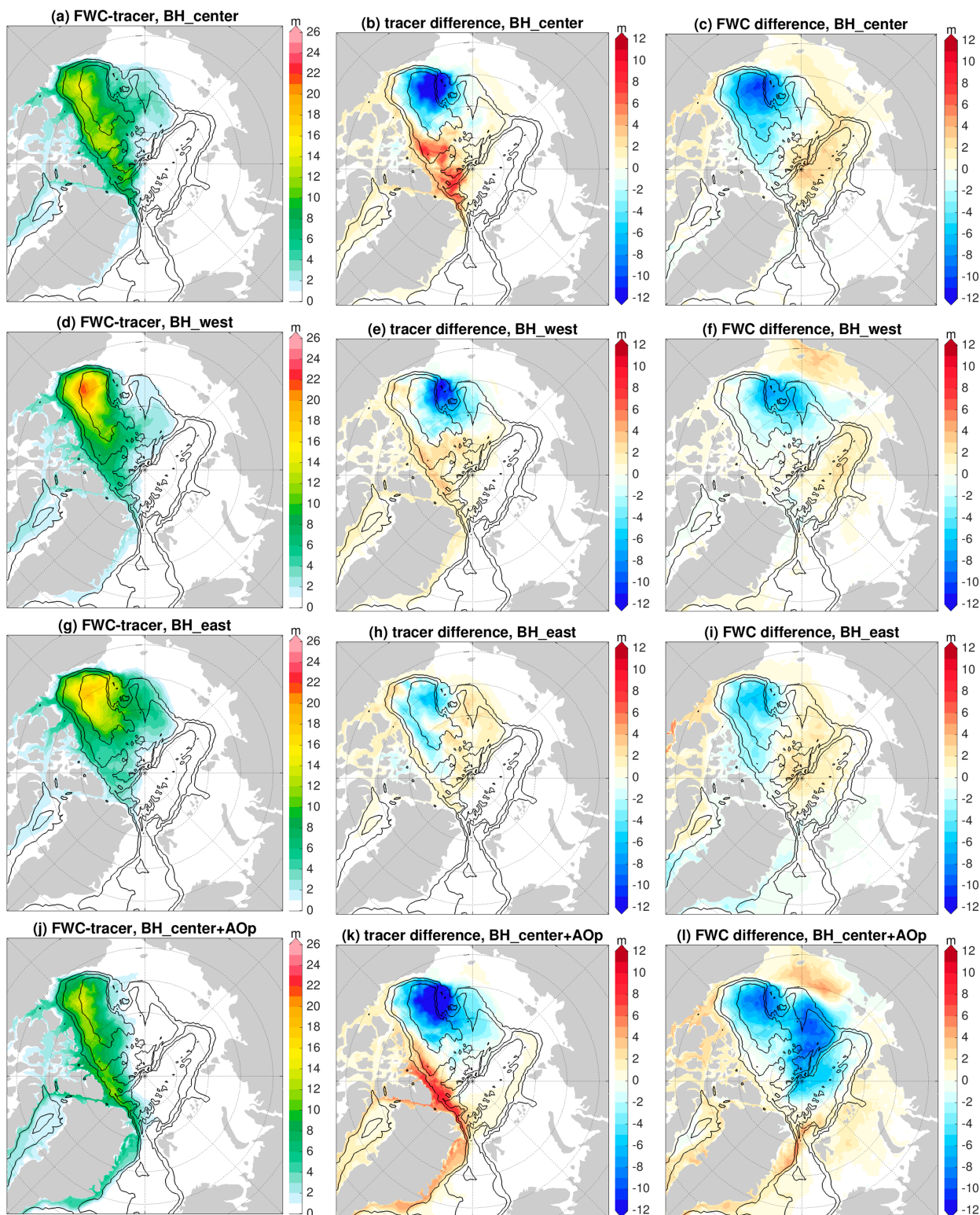


FIG. 5. (a) The FWC-tracer content (m) in the simulation BH_center in the last model year. (b) The difference in the FWC-tracer content between the BH_center run and the control run in the last model year. (c) The difference in the FWC (m) between the BH_center run and the control run in the last model year. The other rows are the same as the top row, but for (d)–(f) the BH_west run, (g)–(i) the BH_east run, and (j)–(l) the BH_center+AOp run.

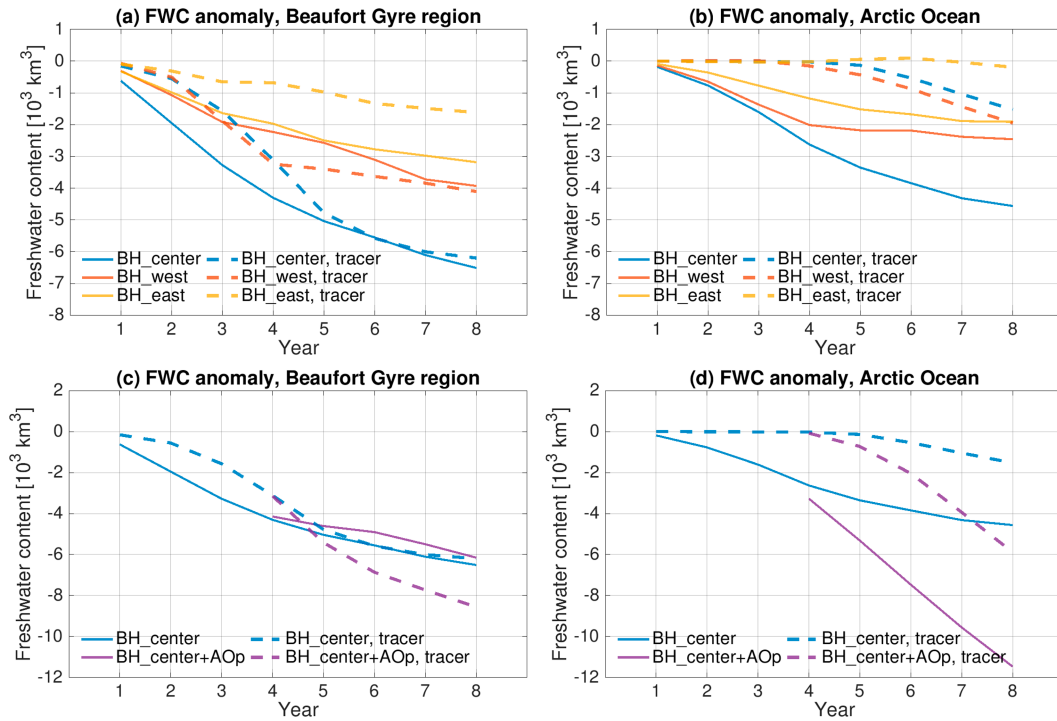


FIG. 6. Anomalies of the FWC and FWC-tracer content in the (left) Beaufort Gyre region and (right) Arctic Ocean. The anomalies are calculated as the difference between the wind-perturbation simulations and the control simulation. FWC is shown with solid lines, and the FWC-tracer content is shown with dashed lines. (a),(b) The impact of cyclonic wind forcing with different locations over the Canada Basin. (c),(d) The impact of positive Arctic Oscillation wind forcing. Note that the y-axis ranges are different in the two rows.

When the imposed cyclonic wind perturbation is shifted westward (in BH_west), the release of the FWC-tracer is attenuated in the eastern Canada Basin while becoming more pronounced in the western Canada Basin (cf. Figs. 5a,d). In this case, the overall release of the FWC-tracer from the Beaufort Gyre region is reduced as indicated by the spatial patterns of the anomalies (Figs. 5b,e), as well as their respective time series (red dashed line and blue dashed line in Fig. 6a). As expected, the reduction in the FWC also follows the westward shift of the wind forcing (Figs. 5c,f), and the overall reduction in the Beaufort Gyre FWC is weakened (red solid line and blue solid line in Fig. 6a).

Qualitatively, shifting the cyclonic wind perturbation eastward (in BH_east) yields contrasting spatial changes in the FWC-tracer and FWC when compared to shifting the wind perturbation westward (cf. Figs. 5h,i with Figs. 5e,f). However, the overall release of both the FWC-tracer and the FWC from the Beaufort Gyre region is the weakest when the wind perturbation is shifted eastward (cf. orange lines with other lines in Fig. 6a). In this particular case, the reduction in the FWC-tracer within the Beaufort Gyre region by the wind perturbation is largely offset by the increase in the FWC-tracer in the Makarov Basin (Fig. 5h). Consequently, the total amount of FWC-tracer in the Arctic Ocean does not exhibit a significant change (orange dashed line in Fig. 6b).

In all three wind-perturbation cases, it is evident that the induced reduction in the FWC-tracer within the Arctic Ocean is less

pronounced than the reduction in the FWC (Fig. 6b). Even after eight model years, a substantial portion of the FWC-tracer released from the Beaufort Gyre remains inside the Arctic Ocean. Specifically, in the BH_center and BH_west experiments, it predominantly lingers north of the Canadian Arctic Archipelago and Greenland, while in the BH_east experiment, it is primarily retained within the Makarov Basin (Figs. 5b,e,h). Quantitatively, comparing the dashed lines in Figs. 6a and 6b, it can be calculated that approximately 75% (BH_center), 50% (BH_west), or 85% (BH_east) of the FWC-tracer released by the wind perturbations remains inside the Arctic Ocean at the end of the simulations. It is important to note that the induced reduction in the FWC within the Arctic Ocean is also milder than that within the Beaufort Gyre region due to the fact that these cyclonic wind perturbations lead to an increase in the FWC in certain Arctic areas outside the Beaufort Gyre (Figs. 5c,f,i).

In the BH_center+AOp experiment, the imposed positive Arctic Oscillation perturbation leads to a notable increase in the release of the FWC-tracer from the Beaufort Gyre region. This effect is particularly pronounced in the northwestern Canada Basin (cf. Fig. 5j with Fig. 5a). The released FWC-tracer due to the positive Arctic Oscillation perturbation is pushed toward Greenland and Canadian Arctic Archipelago, with a fraction of it exported from the Arctic Ocean, particularly through the Fram Strait (cf. Fig. 5k with Fig. 5b). Furthermore, the positive Arctic Oscillation perturbation reduces the FWC in the Makarov Basin and part of the Eurasian Basin (Fig. 5l).

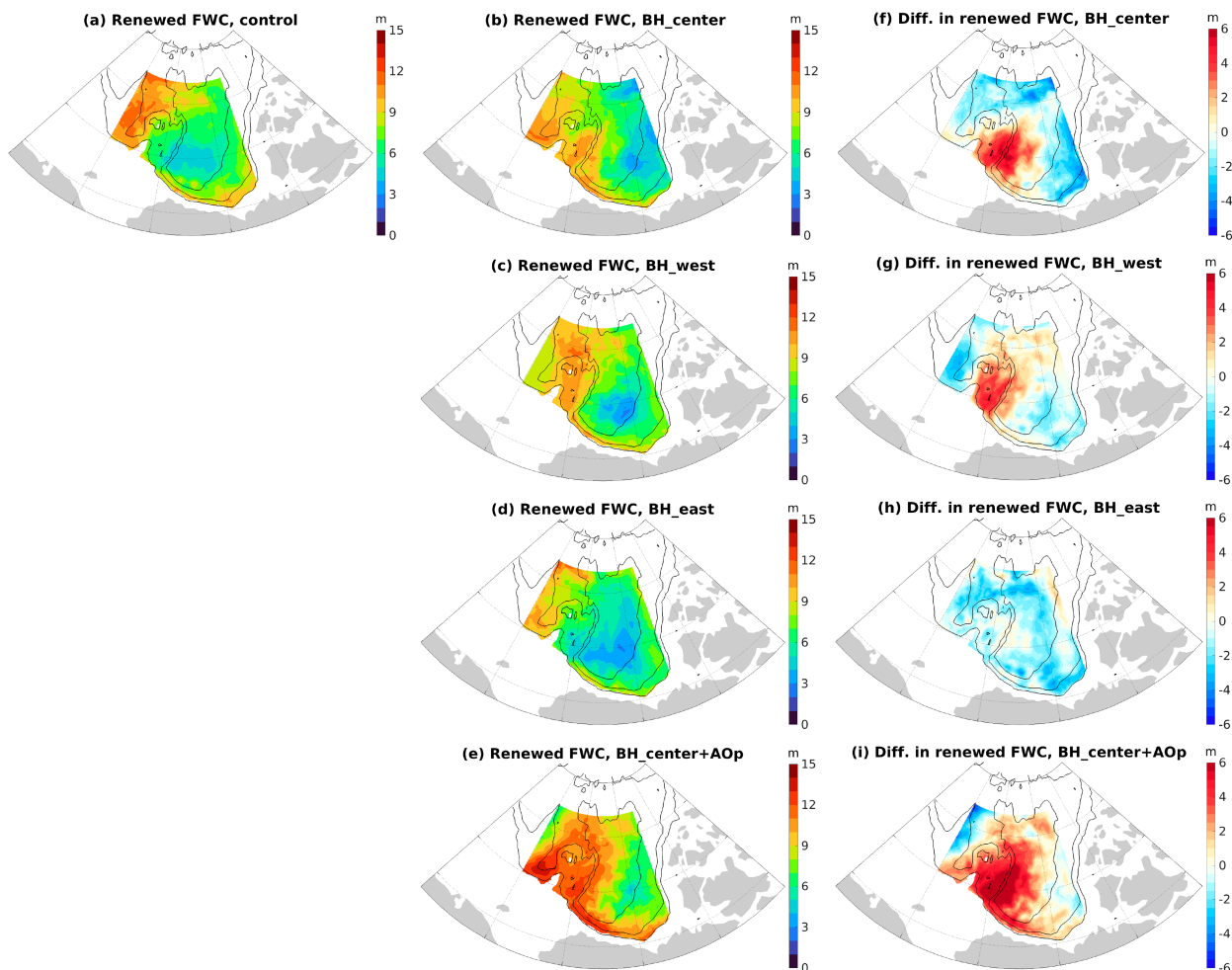


FIG. 7. (a) Renewed FWC (m) in the Beaufort Gyre region in the last model year (2021) in the control simulation. The renewed FWC is defined as the difference between the FWC and the FWC-tracer content. (b)–(e) The renewed FWC in the last model year in different wind-perturbation experiments. (f)–(i) The difference in the renewed FWC between the wind-perturbation experiments and the control simulation (i.e., the middle column minus the left one).

In comparison with BH_center, the release of the FWC-tracer from the Beaufort Gyre region is enhanced by approximately 40% in BH_center+AOp (dashed lines in Fig. 6c), while the reduction in the FWC is slightly weakened (solid line in Fig. 6c). The slight weakening of the reduction is primarily observed in the southern and eastern peripheries of the Canada Basin (cf. Figs. 5l,c). In the presence of the positive Arctic Oscillation perturbation, only about 30% of the FWC-tracer released from the Beaufort Gyre region by the wind perturbations remains within the Arctic Ocean at the end of the simulation (cf. the dashed violet lines in Figs. 6c,d). This fraction is much smaller than in the BH_center experiment, where approximately 75% of the FWC-tracer released by the wind perturbation was retained within the Arctic Ocean, as mentioned earlier. The positive Arctic Oscillation perturbation has a strong impact on reducing the total FWC of the Arctic Ocean, although its effect on the FWC within the Beaufort Gyre region remains relatively modest (cf. the solid violet lines in Figs. 6c,d).

c. Freshwater renewal in the Beaufort Gyre

The difference between the FWC and the FWC-tracer in the Beaufort Gyre region serves as a quantification of the renewed freshwater. Figure 7a depicts the renewed freshwater in the Beaufort Gyre region in 2021 as derived from the control simulation. Freshwater renewal is observed throughout the Beaufort Gyre region; however, it is not uniform in its efficiency. The most pronounced renewal is observed in the western Beaufort Gyre, which aligns with the primary pathway through which Pacific water and Mackenzie River runoff enters the Arctic deep basin (Spall et al. 2018; Lin et al. 2021), as depicted by the spatial pattern of the Beaufort Gyre circulation in Fig. 1c. Additionally, relatively high levels of renewal are detected along the periphery of the gyre, following the anticyclonic gyre circulation. In contrast, the central-south Beaufort Gyre exhibits the weakest renewal.

Imposing the cyclonic Beaufort high wind perturbation effectively alters freshwater renewal (BH_center; Figs. 7b,f). This

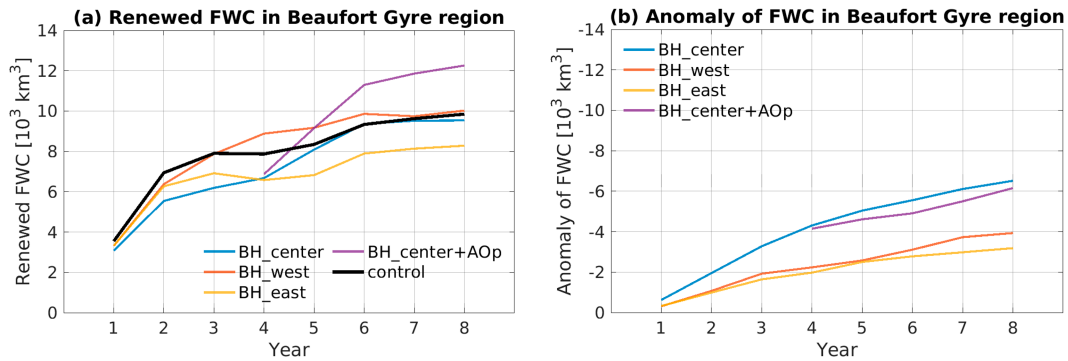


FIG. 8. (a) Renewed FWC in the Beaufort Gyre region, which is defined as the difference between the FWC and the FWC-tracer content. (b) Anomalies of the FWC in the Beaufort Gyre region induced by wind perturbations. The figure indicates that the renewal rate is higher than the release rate even under the strong forcing of cyclonic wind anomalies.

change is characterized by enhanced renewal near the Northwind Ridge and Chukchi Plateau, along with weakened renewal in the western, northern, and eastern peripheries of the gyre (Fig. 7f). The cyclonic wind perturbation deflates the Beaufort Gyre and weakens the anticyclonic Beaufort Gyre circulation, thus allowing for more Pacific water to enter the gyre at a more eastern location (Aksenov et al. 2016; Hu et al. 2019), leading to the enhanced renewal near the Northwind Ridge and Chukchi Plateau. When integrated over the Beaufort Gyre region, the total freshwater renewal does not exhibit a notable change at the end of the simulation compared to the control simulation (blue and black lines in Fig. 8a). However, during the first half of the simulations, the freshwater renewal in BH_center is weaker than that in the control simulation. This difference can be attributed to the rapid response of freshwater release in the periphery of the gyre and the relatively slow eastward shift of the main renewal location. The latter process depends on the strength of the anticyclonic gyre circulation, which weakens over time after the cyclonic wind anomaly is enforced.

Shifting the cyclonic wind perturbation westward (in BH_west) similarly enhances freshwater renewal over the Northwind Ridge and Chukchi Plateau while weakening it in the periphery of the gyre (Figs. 7c,g). However, when compared to the BH_center case, the magnitude of the impact on freshwater renewal is smaller (cf. Figs. 7f,g). Due to the compensation of the positive and negative anomalies, the total Beaufort Gyre renewal in BH_west also remains largely similar to that in the control simulation (Fig. 8a).

Shifting the cyclonic wind perturbation eastward (in BH_east) results in reduced freshwater renewal in most of the Beaufort Gyre area (Figs. 7d,h). The spindown of the Beaufort Gyre is less pronounced in this experiment than in other cases, as indicated by the smaller and more uniform change in the FWC (Fig. 5i). Consequently, the pathway of Pacific water entering the deep basin, thus the location of the strong renewal, is not shifted eastward. As a result, the overall freshwater renewal in the Beaufort Gyre region is the weakest in this experiment (orange line in Fig. 8a).

Imposing the positive Arctic Oscillation wind perturbation in BH_center+AOp effectively strengthens freshwater renewal in

the Beaufort Gyre region (cf. Figs. 7e,i with Figs. 7b,f). This perturbation reduces the FWC-tracer content but results in a slight increase in the FWC within the Beaufort Gyre region (Fig. 6c), consequently reinforcing the renewal process. At the end of the simulations, the freshwater renewal in BH_center+AOp is approximately 20% larger than in the control and BH_center simulations, reflecting the enhanced renewal brought about by the positive Arctic Oscillation wind perturbation.

Our results demonstrate that wind perturbations can influence freshwater renewal within the Beaufort Gyre region, in terms of its spatial distribution and/or the overall efficiency. Regardless of the specific impacts of various wind perturbations, freshwater renewal consistently occurs efficiently. To quantitatively illustrate this efficiency, it is worth noting that in all the cases examined above, the amount of renewed freshwater exceeds the total freshwater released from the Beaufort Gyre region (cf. Figs. 8a,b).

d. Export of Beaufort Gyre freshwater from the Arctic Ocean

Section 3b indicates that a large portion of the FWC-tracer released from the Beaufort Gyre region remains within the Arctic Ocean by the end of the simulations. In this section, we proceed to quantify the export fluxes of the FWC-tracer through the two primary export gateways, namely, the Davis and Fram Straits.

Figure 9a shows the changes in the transport of the FWC-tracer (dashed lines) and changes in the transport of freshwater (solid lines) through the Davis Strait. The behaviors of the two transport types differ substantially. In BH_center experiment (blue lines), the impact of the wind perturbation on FWC-tracer transport is noticeable only starting from the fourth model year. In contrast, freshwater export through the Davis Strait experiences a rapid enhancement already in the first model year, in line with expectation for the applied cyclonic wind perturbation over the Canada Basin. As a result, the increased freshwater export in the first few years does not contain freshwater that was originally present within the Beaufort Gyre at the beginning of the simulation. In the fourth and fifth model years, the FWC-tracer export through the Davis Strait is slightly reduced. Concurrently, more FWC-tracer is advected toward the Fram Strait, as indicated by the enhanced FWC-tracer export in the Fram Strait

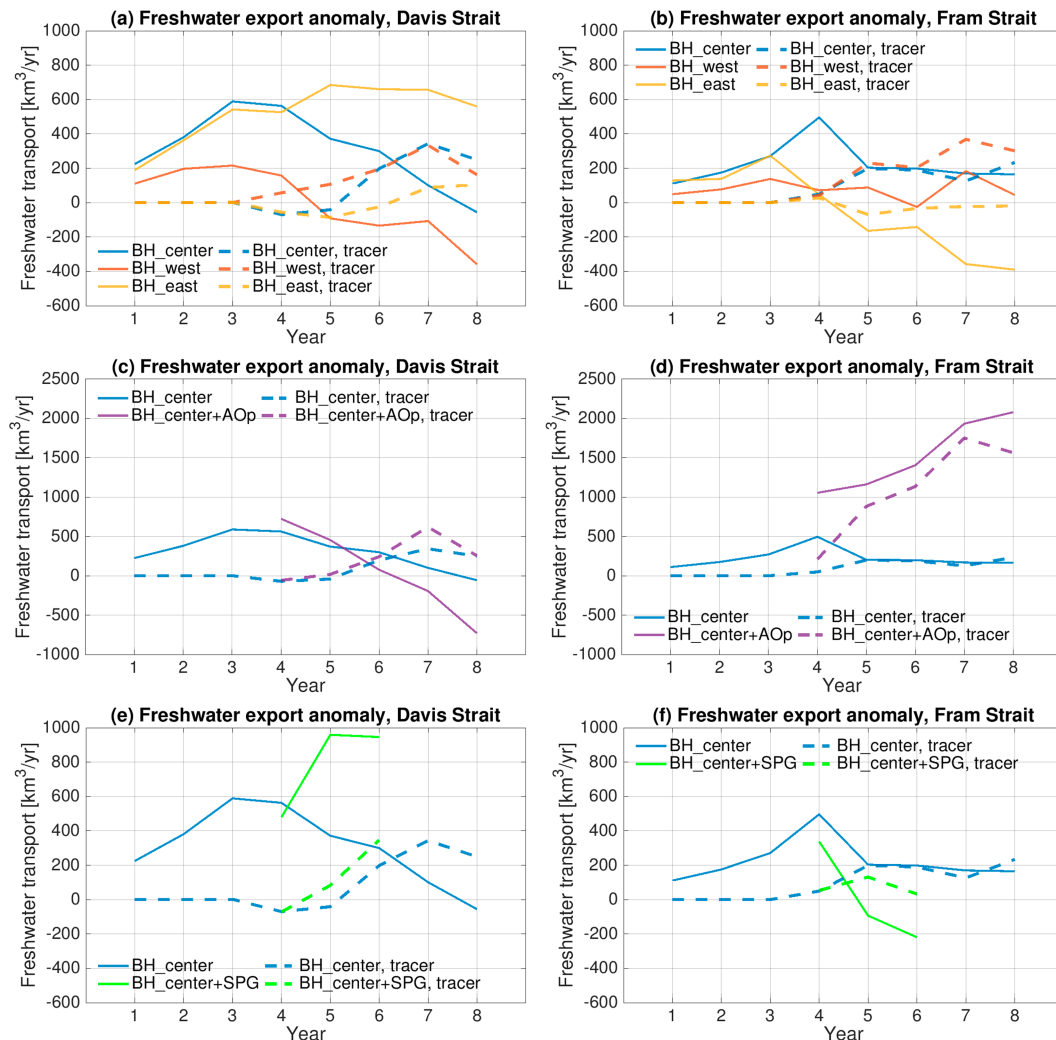


FIG. 9. Anomalies of exports through (left) the Davis Strait and (right) the Fram Strait relative to the control simulation. The anomalies are calculated as the difference between the perturbation simulations and the control simulation. Both the freshwater export (solid) and FWC-tracer export (dashed) are shown. (a),(b) The impact of cyclonic wind forcing with different locations over the Canada Basin. (c),(d) The impact of positive Arctic Oscillation forcing. (e),(f) The impact of the dynamic sea level in the North Atlantic subpolar gyre. Positive values indicate larger export. Note that different y-axis ranges are used.

beginning in the fourth year (dashed blue line in Fig. 9b). Toward the end of the simulation, in the last 3 years, the export of the FWC-tracer through the Davis Strait (dashed blue line in Fig. 9a) is increased, while the freshwater export through the Davis Strait (solid blue line in Fig. 9a) decreases to the point where it falls below the FWC-tracer export. This implies that during this period, the export of freshwater originating from sources other than the original Beaufort Gyre content is eventually reduced. Furthermore, the exports of freshwater and the FWC-tracer through the Fram Strait are very similar in the last four model years (blue lines in Fig. 9b), indicating that the enhanced freshwater export in the Fram Strait predominantly originates from the Beaufort Gyre region.

Shifting the location of the cyclonic wind perturbation has a notable influence on both the exports of the FWC-tracer and

freshwater in the two gateways (Figs. 9a,b). When the wind perturbation is shifted westward (in BH_west), the increase in freshwater export through the Davis Strait is reduced in the first few model years, and it even becomes negative starting from the fifth year (solid red line in Fig. 9a). In contrast, the export of the FWC-tracer in the Davis Strait is enhanced already from the fourth model year in this experiment (dashed red line in Fig. 9a). This stronger export of the FWC-tracer is consistent with the lower FWC-tracer content in the Arctic Ocean in this experiment compared to BH_center (Fig. 6b). The changes in freshwater export and FWC-tracer export are not consistent throughout this simulation for both the gateways.

Shifting the location of the cyclonic wind perturbation eastward (in BH_east) results in a significant enhancement of freshwater export through the Davis Strait in all years.

However, this enhancement is partially offset by a reduction in the freshwater export through the Fram Strait (solid orange lines in Figs. 9a,b). This compensation suggests a shift in the export of freshwater between the two gateways. The effect of this wind perturbation on freshwater exports, with its center closer to the Canadian Arctic Archipelago, qualitatively resembles that of the negative Arctic dipole anomaly (Wang et al. 2023), which has one of its active centers close to the Canadian Arctic Archipelago and north Greenland (Wu et al. 2006). Notably, the changes in the FWC-tracer exports are the smallest in BH_east.

The addition of the positive Arctic Oscillation wind perturbation has a profound impact on freshwater exports in the two gateways (in BH_center+AOp; solid violet lines in Figs. 9c,d). Specifically, it substantially increases freshwater export in the Fram Strait and reduces freshwater export in the Davis Strait (after a small adjustment in the first 2 years), as found in previous studies (Steele et al. 2004; Wang et al. 2021). While the FWC-tracer export is not altered much in the Davis Strait, it experiences a considerable increase in the Fram Strait (dashed violet lines in Figs. 9c,d). The increase in the Fram Strait freshwater export can primarily be attributed to the freshwater originating from the Beaufort Gyre, as indicated by the FWC-tracer flux. This is consistent with the substantial reduction in the FWC-tracer content in the Arctic Ocean in this simulation (Fig. 6d).

In the BH_center+SPG experiment, the sea level in the subpolar gyre (60° – 15° W, 53° – 64° N) in 2017–19 is reduced compared to that in the control simulation and observations (Fig. 10). Consequently, compared with BH_center, freshwater export in the Davis Strait experiences a substantial increase, while freshwater export in the Fram Strait is reduced (solid green lines in Figs. 9e,f). The changes in the FWC-tracer export have the same sign as in the freshwater export, with increases in the Davis Strait and decreases in the Fram Strait (dashed green lines in Figs. 9e,f) compared with BH_center. The magnitudes of the change (about $150 \text{ km}^3 \text{ yr}^{-1}$) in the FWC-tracer export induced by the sea level change in the subpolar gyre are much smaller than those of the changes in freshwater export, but they are on the same order as the changes in the FWC-tracer export induced by the cyclonic Beaufort high wind perturbations shown in Figs. 9a and 9b.

4. Discussion

Our experiments described above reveal that freshwater renewal occurs in the Beaufort Gyre region when the Beaufort Gyre releases freshwater under the cyclonic wind forcing anomalies. An additional experiment (BHp) driven by an anticyclonic wind perturbation complements the understanding and shows that freshwater renewal is a general process occurring in any wind conditions (Fig. 11). Under the anticyclonic wind perturbation, more FWC-tracer accumulates around the Chukchi Plateau (Fig. 11a) in comparison with the control simulation. As expected, the FWC increases in the Beaufort Gyre region under the anticyclonic wind perturbation (Fig. 11b). The accumulation of freshwater leads to pronounced freshwater renewal in the Beaufort Gyre region (Fig. 11c), more than in other simulations nearly at all places of the Beaufort Gyre region. Due to the

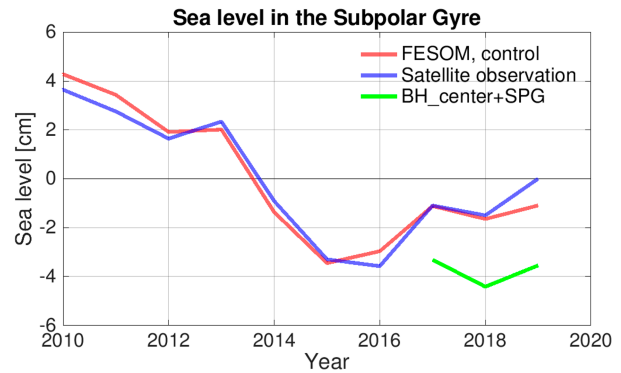


FIG. 10. Sea surface height (SSH) anomaly in the North Atlantic subpolar gyre in satellite observations (Pujol et al. 2016), the FESOM control simulation, and the BH_center+SPG perturbation experiment. In this perturbation experiment, the atmospheric forcing outside the Arctic was replaced by that from 2014 to 2016 in order to retain the low sea level in the subpolar gyre. The purpose is to demonstrate the impact of the sea level south of Greenland on the routing of the freshwater export as shown in Figs. 9e and 9f.

accumulation of freshwater originally located inside the Beaufort Gyre into the area of the Chukchi Plateau as indicated by the FWC-tracer anomaly (Fig. 11a), the freshwater renewal is relatively low in this central area (Fig. 11c). Compared to the control simulation, freshwater renewal in BHp is enhanced everywhere in the Beaufort Gyre region (Fig. 11d). The enhancement is more pronounced in the eastern and southern parts of the gyre, consistent with the anticyclonic pathway of freshwater circulation.

The freshwater renewal studied in this paper should not be confused with “ventilation.” Ventilation usually refers to processes that transfer waters that have recently been in contact with the atmosphere (sometimes called young waters) into the ocean interior, such as wind-driven subduction of surface water or intrusion of near-surface water through Barrow Canyon into the halocline (Timmermans et al. 2014, 2017, 2018; Spall et al. 2018; MacKinnon et al. 2021). Freshwater renewal rather refers to the addition of freshwater into the Beaufort Gyre since a specified time. The renewed freshwater could be supplied by ventilation processes, while it can also be added directly to the gyre surface (e.g., ice meltwater) or advected laterally into the Beaufort Gyre through the gyre’s northern and eastern boundaries. It does not distinguish young and old waters relative to the time of their contact with the atmosphere. To study ventilation processes, using additional tracers (such as age tracer or tracers representing specific water masses) in model simulations would be helpful. Further studies are also needed to better understand relative contributions of different sources to the freshwater renewal of the Beaufort Gyre.

The results obtained in this study are subject to model uncertainty. Although the model configuration used in this study can reasonably reproduce the observed changes in Arctic sea ice and the FWC (Q. Wang et al. 2018, 2020; Wang 2021; Wang and Danilov 2022), its resolution cannot fully resolve mesoscale eddies and thus the impacts of eddies on freshwater transport. Furthermore, the most efficient freshwater renewal in the control simulation is at the Chukchi Abyssal Plain, west of the Chukchi

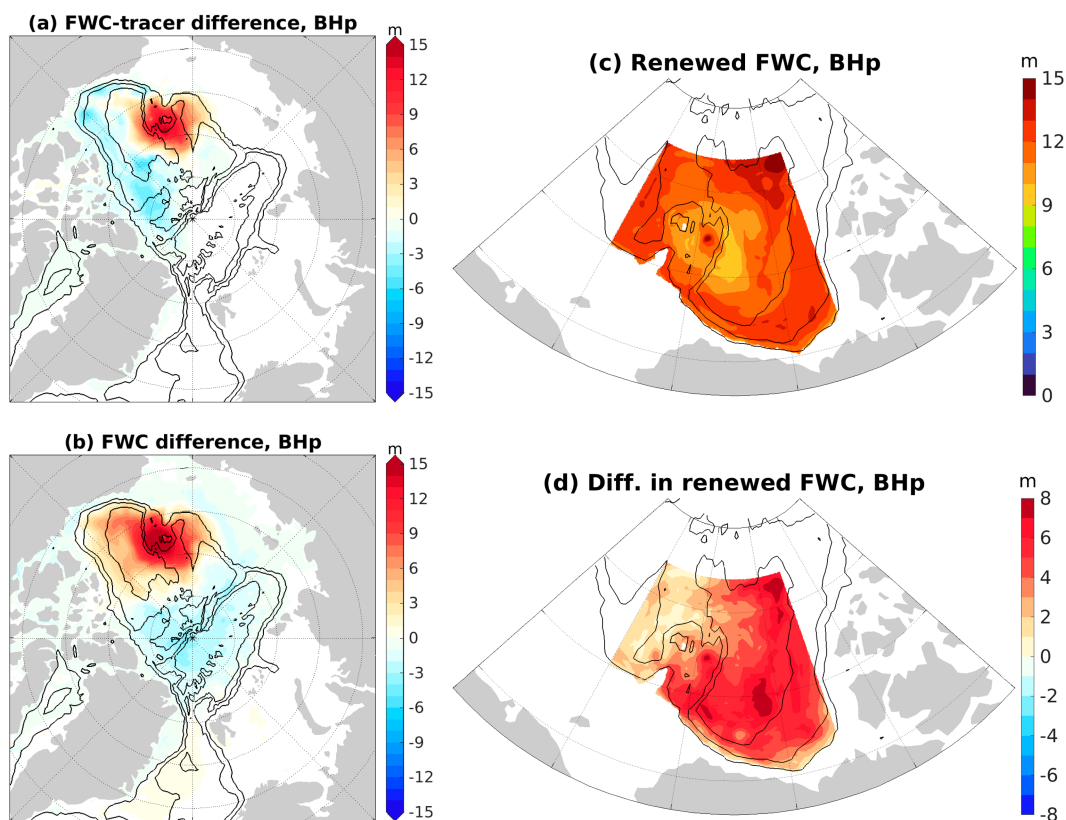


FIG. 11. (a) The difference in the FWC-tracer content (m) between the BHp run and the control run in the last model year. (b) The difference in the FWC (m) between the BHp run and the control run in the last model year. (c) Renewed FWC in the Beaufort Gyre region in the last model year in the BHp run. (d) The difference in the renewed FWC between the BHp run and the control run.

Plateau (Fig. 7a), while observations indicate that Pacific water and Mackenzie River water very possibly traverse the Chukchi Plateau (Boury et al. 2020; Lin et al. 2021). This discrepancy could be due to the overestimated size of the Beaufort Gyre on the western side in the simulation (Fig. 1c). These model deficiencies can influence the quantitative results. Moreover, the quantitative results are also subject to the simulation period used in this study. If the FWC-tracer is initialized in a different year, a different amount of the initial FWC-tracer may lead to quantitative differences in the response of the FWC-tracer to wind perturbations. Hence, it is essential to view this study primarily as a process-oriented investigation using model resolution affordable so far, aiming to understand the intricacies of some of the dynamics involved. For this purpose, the applied wind perturbations are idealized, which simplifies the interpretation of the simulation results.

The FWC is defined relative to the chosen reference salinity [Eq. (1)]. Using a different reference salinity can lead to different mean values of the FWC, but our tests show that the variability of the FWC is not very sensitive to the reference salinity. Furthermore, the chosen reference salinity is close to the mean salinity of the Arctic Ocean, so the FWC reflects the amount of freshwater relative to the mean state of the Arctic Ocean. This reference salinity was also used in observations (Proshutinsky et al. 2019) and other model studies. Using the same value allows for direct intercomparisons. We introduced an FWC-tracer using the same

reference salinity in this paper. The consistent definition provides the possibility to explore the processes of freshwater export and renewal.

5. Conclusions

This paper explores the release and renewal of Beaufort Gyre freshwater under various wind-perturbation scenarios (Table 1). We introduced an FWC-tracer to represent freshwater originally located within the Beaufort Gyre region at the beginning of the wind-perturbation experiments. The results are summarized below.

- Applying a cyclonic wind perturbation over the Canada Basin (associated with a negative anomaly of the Beaufort high sea level pressure) leads to a notable reduction in the FWC and FWC-tracer in the Beaufort Gyre. The FWC-tracer released from the Beaufort Gyre accumulates north of the Canadian Arctic Archipelago and Greenland, with export on both sides of Greenland. Shifting the cyclonic wind perturbation westward or eastward reduces its efficiency in releasing FWC-tracer and freshwater from the Beaufort Gyre. In these wind-perturbation cases, a significant portion of the FWC-tracer released from the Beaufort Gyre still remains inside the Arctic Ocean after eight model years.

- Adding an additional positive Arctic Oscillation perturbation increases the release of the FWC-tracer from the Beaufort Gyre by approximately 40%, mainly through the impact in the northwestern Canada Basin. The positive Arctic Oscillation perturbation also considerably reduces both the FWC-tracer and FWC in the Arctic Ocean. In the presence of the positive Arctic Oscillation perturbation, only about 30% of the FWC-tracer released from the Beaufort Gyre region by the applied wind perturbation remains within the Arctic Ocean by the end of the simulation, a smaller fraction compared to the case when it is absent (75%).
- Freshwater renewal in the Beaufort Gyre occurs universally, being distributed throughout the Beaufort Gyre but more substantial in the western part, which aligns with the primary Pacific water and Mackenzie River runoff pathway in the model. Applying the cyclonic wind perturbation over the Canada Basin enhances freshwater renewal near the Northwind Ridge but weakens it in the gyre's periphery, so the total freshwater renewal remains relatively unchanged.
- When the cyclonic wind perturbation is shifted westward, the impact of the wind perturbation on freshwater renewal remains similar in pattern while being smaller in magnitude. In this case, the total freshwater renewal in the gyre is also similar to the control simulation. In contrast, shifting the wind perturbation eastward reduces the overall renewal. Applying an additional positive Arctic Oscillation perturbation strengthens freshwater renewal, resulting in approximately 20% more renewal by the end of the simulation. Overall, wind perturbations can influence freshwater renewal in the Beaufort Gyre region, affecting its spatial distribution and/or overall efficiency. Importantly, regardless of the specific impacts of different cyclonic wind perturbations, freshwater renewal consistently occurs efficiently, with the amount of renewed freshwater surpassing the total released freshwater from the Beaufort Gyre region.
- When the Beaufort Gyre gathers freshwater under a strong anticyclonic wind perturbation, accumulation of new water occurs across the entire gyre, but the central region of the gyre has a relatively lower renewal rate than the surrounding areas because freshwater originally located inside the gyre accumulates into this central region.
- We further investigated the export of Beaufort Gyre freshwater from the Arctic Ocean via the Davis and Fram Straits. When applying the cyclonic wind perturbation over the Canada Basin, freshwater export through the Davis Strait increases rapidly, while FWC-tracer export shows a delayed rise, suggesting that freshwater from sources other than the original Beaufort Gyre content gets exported first. In the last few model years, when the anomaly of FWC-tracer export through the Davis Strait is high, the anomaly of freshwater export through the Davis Strait actually drops below that of the FWC-tracer export. Exports of freshwater and FWC-tracer through the Fram Strait are similar in the second half of the simulation period, indicating that freshwater export predominantly originated from the Beaufort Gyre.
- Shifting the cyclonic wind perturbation westward reduces the increase in freshwater export through both straits and enhances FWC-tracer export in some of the model years (compared

to the case when the perturbation is not shifted). Shifting the wind perturbation eastward significantly enhances freshwater export through the Davis Strait while offsetting it with reduced freshwater export through the Fram Strait, resembling the effect of a negative Arctic dipole anomaly. The changes in FWC-tracer exports in the two gateways induced by the wind perturbations are the smallest when the wind perturbation is shifted eastward. The addition of the positive Arctic Oscillation wind perturbation substantially increases freshwater export in the Fram Strait and reduces it in the Davis Strait. In this case, the FWC-tracer export remains similar in the Davis Strait but experiences a significant increase in the Fram Strait. Last, we address that both the exports of freshwater and FWC-tracer can be strongly influenced by dynamic sea level south of Greenland. Reduced dynamic sea level in the subpolar gyre leads to increased freshwater and FWC-tracer exports through the Davis Strait and decreased exports through the Fram Strait.

We discovered that freshwater renewal in the Beaufort Gyre region is a consistently efficient process, regardless of whether the gyre is in a phase of releasing or accumulating freshwater. However, this renewal process exhibits spatial variability, which can be influenced by wind forcing associated with various atmospheric modes. The precise location of the maximum and the magnitude of the renewal are subject to the interplay of wind forcing and gyre circulation patterns.

The Beaufort Gyre stands as the largest freshwater reservoir within the Arctic Ocean, making its status and potential freshwater release a matter of significant climate concern. This study reveals that it takes 3–4 years for the freshwater from the Beaufort Gyre region to reach the Davis and Fram Straits. A cyclonic wind anomaly, such as during a negative phase of the Beaufort high anomaly, can lead to the release of freshwater from the Beaufort Gyre. However, in certain conditions, only a relatively small portion of the released freshwater finds its way to the North Atlantic within an 8-yr period, with the majority remaining within the Arctic Ocean. During the initial years after imposing a cyclonic wind anomaly in the Canada Basin, the increased freshwater exports through the two gateways primarily consist of freshwater not originating from the Beaufort Gyre. Depending on specific wind conditions, it is possible that the overall freshwater export may decrease to levels lower than usual when the freshwater originating from the Beaufort Gyre region eventually reaches the Arctic gateways. Our findings suggest the importance of considering both the freshwater in the Beaufort Gyre and other freshwater sources when assessing the role of Arctic export in the climate system. It is also necessary to account for overall wind and thermal forcing conditions in the Arctic and North Atlantic as well when seeking to understand and predict changes in Arctic freshwater exports through the two gateways.

Acknowledgments. This work is supported by the Helmholtz Climate Initiative REKLIM (Regional Climate Change and Human) and the EPICA project in the research theme “MARE:N—Polarforschung/MOSAIC” funded by the German Federal Ministry for Education and Research with funding

03F0889A. The author is grateful to the reviewers and the editor for their helpful comments.

Data availability statement. Model data used to produce figures in this paper are available at <https://doi.org/10.5281/zenodo.8320306> as cited in Wang (2023).

REFERENCES

- Aagaard, K., J. H. Swift, and E. C. Carmack, 1985: Thermohaline circulation in the Arctic Mediterranean Seas. *J. Geophys. Res.*, **90**, 4833–4846, <https://doi.org/10.1029/JC090iC03p04833>.
- Aksenov, Y., S. Bacon, A. C. Coward, and N. P. Holliday, 2010: Polar outflow from the Arctic Ocean: A high resolution model study. *J. Mar. Syst.*, **83**, 14–37, <https://doi.org/10.1016/j.jmarsys.2010.06.007>.
- , and Coauthors, 2016: Arctic pathways of Pacific water: Arctic Ocean Model intercomparison experiments. *J. Geophys. Res. Oceans*, **121**, 27–59, <https://doi.org/10.1002/2015JC011299>.
- Armitage, T. W. K., S. Bacon, A. L. Ridout, A. A. Petty, S. Wolbach, and M. Tsamados, 2017: Arctic Ocean surface geostrophic circulation 2003–2014. *Cryosphere*, **11**, 1767–1780, <https://doi.org/10.5194/te-11-1767-2017>.
- Azetsu-Scott, K., and Coauthors, 2010: Calcium carbonate saturation states in the waters of the Canadian Arctic Archipelago and the Labrador Sea. *J. Geophys. Res.*, **115**, C11021, <https://doi.org/10.1029/2009JC005917>.
- Boury, S., and Coauthors, 2020: Whither the Chukchi Slope Current? *J. Phys. Oceanogr.*, **50**, 1717–1732, <https://doi.org/10.1175/JPO-D-19-0273.1>.
- Carmack, E. C., and Coauthors, 2016: Freshwater and its role in the Arctic Marine System: Sources, disposition, storage, export, and physical and biogeochemical consequences in the Arctic and global oceans. *J. Geophys. Res. Biogeosci.*, **121**, 675–717, <https://doi.org/10.1002/2015JG003140>.
- Condron, A., P. Winsor, C. Hill, and D. Menemenlis, 2009: Simulated response of the Arctic freshwater budget to extreme NAO wind forcing. *J. Climate*, **22**, 2422–2437, <https://doi.org/10.1175/2008JCL2626.1>.
- Cornish, S. B., Y. Kostov, H. L. Johnson, and C. Lique, 2020: Response of Arctic freshwater to the Arctic Oscillation in coupled climate models. *J. Climate*, **33**, 2533–2555, <https://doi.org/10.1175/JCLI-D-19-0685.1>.
- Curry, B., C. M. Lee, B. Petrie, R. E. Moritz, and R. Kwok, 2014: Multiyear volume, liquid freshwater, and sea ice transports through Davis Strait, 2004–2010. *J. Phys. Oceanogr.*, **44**, 1244–1266, <https://doi.org/10.1175/JPO-D-13-0177.1>.
- Danilov, S., Q. Wang, R. Timmermann, N. Iakovlev, D. Sidorenko, M. Kimmritz, T. Jung, and J. Schroeter, 2015: Finite-Element Sea Ice Model (FESIM), version 2. *Geosci. Model Dev.*, **8**, 1747–1761, <https://doi.org/10.5194/gmd-8-1747-2015>.
- de Steur, L., C. Peralta-Ferriz, and O. Pavlova, 2018: Freshwater export in the East Greenland Current freshens the North Atlantic. *Geophys. Res. Lett.*, **45**, 13 359–13 366, <https://doi.org/10.1029/2018GL080207>.
- Giles, K. A., S. W. Laxon, A. L. Ridout, D. J. Wingham, and S. Bacon, 2012: Western Arctic Ocean freshwater storage increased by wind-driven spin-up of the Beaufort Gyre. *Nat. Geosci.*, **5**, 194–197, <https://doi.org/10.1038/ngeo1379>.
- Hu, X., P. G. Myers, and Y. Lu, 2019: Pacific water pathway in the Arctic Ocean and Beaufort Gyre in two simulations with different horizontal resolutions. *J. Geophys. Res. Oceans*, **124**, 6414–6432, <https://doi.org/10.1029/2019JC015111>.
- Jahn, A., B. Tremblay, L. A. Mysak, and R. Newton, 2010: Effect of the large-scale atmospheric circulation on the variability of the Arctic Ocean freshwater export. *Climate Dyn.*, **34**, 201–222, <https://doi.org/10.1007/s00382-009-0558-z>.
- Karpouzoglou, T., L. de Steur, L. H. Smedsrud, and H. Sumata, 2022: Observed changes in the Arctic freshwater outflow in Fram Strait. *J. Geophys. Res. Oceans*, **127**, e2021JC018122, <https://doi.org/10.1029/2021JC018122>.
- Krishfield, R. A., A. Proshutinsky, K. Tateyama, W. J. Williams, E. C. Carmack, F. A. McLaughlin, and M.-L. Timmermans, 2014: Deterioration of perennial sea ice in the Beaufort Gyre from 2003 to 2012 and its impact on the oceanic freshwater cycle. *J. Geophys. Res. Oceans*, **119**, 1271–1305, <https://doi.org/10.1002/2013JC008999>.
- Lin, P., R. S. Pickart, K. Vage, and J. Li, 2021: Fate of warm Pacific water in the Arctic Basin. *Geophys. Res. Lett.*, **48**, e2021GL094693, <https://doi.org/10.1029/2021GL094693>.
- , —, H. Heorton, M. Tsamados, M. Itoh, and T. Kikuchi, 2023: Recent state transition of the Arctic Ocean’s Beaufort Gyre. *Nat. Geosci.*, **16**, 485–491, <https://doi.org/10.1038/s41561-023-01184-5>.
- Lique, C., A. M. Treguier, M. Scheinert, and T. Penduff, 2009: A model-based study of ice and freshwater transport variability along both sides of Greenland. *Climate Dyn.*, **33**, 685–705, <https://doi.org/10.1007/s00382-008-0510-7>.
- MacKinnon, J. A., and Coauthors, 2021: A warm jet in a cold ocean. *Nat. Commun.*, **12**, 2418, <https://doi.org/10.1038/s41467-021-22505-5>.
- Maslowski, W., B. Newton, A. Schlosser, P. Semtner, and D. Martinson, 2000: Modeling recent climate variability in the Arctic Ocean. *Geophys. Res. Lett.*, **27**, 3743–3746, <https://doi.org/10.1029/1999GL011227>.
- McPhee, M. G., A. Proshutinsky, J. H. Morison, M. Steele, and M. B. Alkire, 2009: Rapid change in freshwater content of the Arctic Ocean. *Geophys. Res. Lett.*, **36**, L10602, <https://doi.org/10.1029/2009GL037525>.
- Morison, J., R. Kwok, C. Peralta-Ferriz, M. Alkire, I. Rigor, R. Andersen, and M. Steele, 2012: Changing Arctic Ocean freshwater pathways. *Nature*, **481**, 66–70, <https://doi.org/10.1038/nature10705>.
- , and Coauthors, 2021: The cyclonic mode of Arctic Ocean circulation. *J. Phys. Oceanogr.*, **51**, 1053–1075, <https://doi.org/10.1175/JPO-D-20-0190.1>.
- Proshutinsky, A., R. H. Bourke, and F. A. McLaughlin, 2002: The role of the Beaufort Gyre in Arctic climate variability: Seasonal to decadal climate scales. *Geophys. Res. Lett.*, **29**, 2100, <https://doi.org/10.1029/2002GL015847>.
- , and Coauthors, 2009: Beaufort Gyre freshwater reservoir: State and variability from observations. *J. Geophys. Res.*, **114**, C00A10, <https://doi.org/10.1029/2008JC005104>.
- , D. Dukhovskoy, M. Timmermans, R. Krishfield, and J. Bamber, 2015: Arctic circulation regimes. *Philos. Trans. Roy. Soc.*, **A373**, 20140160, <https://doi.org/10.1098/rsta.2014.0160>.
- , and Coauthors, 2019: Analysis of the Beaufort Gyre freshwater content in 2003–2018. *J. Geophys. Res. Oceans*, **124**, 9658–9689, <https://doi.org/10.1029/2019JC015281>.
- , R. Krishfield, and M. L. Timmermans, 2020: Introduction to special collection on Arctic Ocean Modeling and Observational Synthesis (FAMOS) 2: Beaufort Gyre phenomenon. *J. Geophys. Res. Oceans*, **125**, e2019JC015400, <https://doi.org/10.1029/2019JC015400>.

- Pujol, M.-I., Y. Faugère, G. Taburet, S. Dupuy, C. Pelloquin, M. Ablain, and N. Picot, 2016: DUACS DT2014: The new multi-mission altimeter data set reprocessed over 20 years. *Ocean Sci.*, **12**, 1067–1090, <https://doi.org/10.5194/os-12-1067-2016>.
- Regan, H. C., C. Lique, and T. W. K. Armitage, 2019: The Beaufort Gyre extent, shape, and location between 2003 and 2014 from satellite observations. *J. Geophys. Res. Oceans*, **124**, 844–862, <https://doi.org/10.1029/2018JC014379>.
- Rudels, B., 1989: The formation of polar surface water, the ice export and the exchanges through the Fram Strait. *Prog. Oceanogr.*, **22**, 205–248, [https://doi.org/10.1016/0079-6611\(89\)90013-X](https://doi.org/10.1016/0079-6611(89)90013-X).
- Serreze, M. C., and Coauthors, 2006: The large-scale freshwater cycle of the Arctic. *J. Geophys. Res.*, **111**, C11010, <https://doi.org/10.1029/2005JC003424>.
- Spall, M. A., R. S. Pickart, M. Li, M. Itoh, P. Lin, T. Kikuchi, and Y. Qi, 2018: Transport of Pacific water into the Canada Basin and the formation of the Chukchi Slope Current. *J. Geophys. Res. Oceans*, **123**, 7453–7471, <https://doi.org/10.1029/2018JC013825>.
- Steele, M., R. Morley, and W. Ermold, 2001: PHC: A global ocean hydrography with a high-quality Arctic Ocean. *J. Climate*, **14**, 2079–2087, [https://doi.org/10.1175/1520-0442\(2001\)014<2079:PAGOHW>2.0.CO;2](https://doi.org/10.1175/1520-0442(2001)014<2079:PAGOHW>2.0.CO;2).
- , J. Morison, W. Ermold, I. Rigor, M. Ortmeyer, and K. Shimada, 2004: Circulation of summer Pacific halocline water in the Arctic Ocean. *J. Geophys. Res.*, **109**, C02027, <https://doi.org/10.1029/2003JC002009>.
- Thompson, D. W. J., and J. M. Wallace, 1998: The Arctic Oscillation signature in the wintertime geopotential height and temperature fields. *Geophys. Res. Lett.*, **25**, 1297–1300, <https://doi.org/10.1029/98GL00950>.
- Timmermans, M.-L., and J. M. Toole, 2023: The Arctic Ocean's Beaufort Gyre. *Annu. Rev. Mar. Sci.*, **15**, 223–248, <https://doi.org/10.1146/annurev-marine-032122-012034>.
- , and Coauthors, 2014: Mechanisms of Pacific summer water variability in the Arctic's central Canada Basin. *J. Geophys. Res. Oceans*, **119**, 7523–7548, <https://doi.org/10.1002/2014JC010273>.
- , J. Marshall, A. Proshutinsky, and J. Scott, 2017: Seasonally derived components of the Canada Basin halocline. *Geophys. Res. Lett.*, **44**, 5008–5015, <https://doi.org/10.1002/2017GL073042>.
- , J. Toole, and R. Krishfield, 2018: Warming of the interior Arctic Ocean linked to sea ice losses at the basin margins. *Sci. Adv.*, **4**, eaat6773, <https://doi.org/10.1126/sciadv.aat6773>.
- Tsujino, H., and Coauthors, 2018: JRA-55 based surface dataset for driving ocean–sea-ice models (JRA55-do). *Ocean Modell.*, **130**, 79–139, <https://doi.org/10.1016/j.ocemod.2018.07.002>.
- Wang, H., S. Legg, and R. Hallberg, 2018: The effect of Arctic freshwater pathways on North Atlantic convection and the Atlantic meridional overturning circulation. *J. Climate*, **31**, 5165–5188, <https://doi.org/10.1175/JCLI-D-17-0629.1>.
- Wang, Q., 2021: Stronger variability in the Arctic Ocean induced by sea ice decline in a warming climate: Freshwater storage, dynamic sea level and surface circulation. *J. Geophys. Res. Oceans*, **126**, e2020JC016886, <https://doi.org/10.1029/2020JC016886>.
- , 2023: Model data of Beaufort Gyre release and ventilation study. Zenodo, accessed 5 February 2024, <https://doi.org/10.5281/zenodo.8320306>.
- , and S. Danilov, 2022: A synthesis of the upper Arctic Ocean circulation during 2000–2019: Understanding the roles of wind forcing and sea ice decline. *Front. Mar. Sci.*, **9**, 863204, <https://doi.org/10.3389/fmars.2022.863204>.
- , —, D. Sidorenko, R. Timmermann, C. Wekerle, X. Wang, T. Jung, and J. Schröter, 2014: The Finite Element Sea Ice-Ocean Model (FESOM) v.1.4: Formulation of an ocean general circulation model. *Geosci. Model Dev.*, **7**, 663–693, <https://doi.org/10.5194/gmd-7-663-2014>.
- , C. Wekerle, S. Danilov, N. Koldunov, D. Sidorenko, D. Sein, B. Rabe, and T. Jung, 2018: Arctic sea ice decline significantly contributed to the unprecedented liquid freshwater accumulation in the Beaufort Gyre of the Arctic Ocean. *Geophys. Res. Lett.*, **45**, 4956–4964, <https://doi.org/10.1029/2018GL077901>.
- , and Coauthors, 2020: Intensification of the Atlantic water supply to the Arctic Ocean through Fram Strait induced by Arctic sea ice decline. *Geophys. Res. Lett.*, **47**, e2019GL086682, <https://doi.org/10.1029/2019GL086682>.
- , S. Danilov, D. Sidorenko, and X. Wang, 2021: Circulation pathways and exports of Arctic river runoff influenced by atmospheric circulation regimes. *Front. Mar. Sci.*, **8**, 707593, <https://doi.org/10.3389/fmars.2021.707593>.
- , Q. Shu, S. Danilov, and D. Sidorenko, 2022: An extreme event of enhanced Arctic Ocean export west of Greenland caused by the pronounced dynamic sea level drop in the North Atlantic subpolar gyre in the mid-to-late 2010s. *Environ. Res. Lett.*, **17**, 044046, <https://doi.org/10.1088/1748-9326/ac5562>.
- , and Coauthors, 2023: A review of Arctic–subarctic ocean linkages: Past changes, mechanisms, and future projections. *Ocean-Land-Atmos. Res.*, **2**, 0013, <https://doi.org/10.34133/olar.0013>.
- Weijer, W., and Coauthors, 2019: Stability of the Atlantic meridional overturning circulation: A review and synthesis. *J. Geophys. Res. Oceans*, **124**, 5336–5375, <https://doi.org/10.1029/2019JC015083>.
- , T. Haine, A. Siddiqui, W. Cheng, M. Veneziani, and P. Kurtakoti, 2022: Interactions between the Arctic Mediterranean and the Atlantic meridional overturning circulation: A review. *Oceanography*, **35** (3–4), 118–127, <https://doi.org/10.5670/oceanog.2022.130>.
- Wu, B., J. Wang, and J. E. Walsh, 2006: Dipole anomaly in the winter Arctic atmosphere and its association with sea ice motion. *J. Climate*, **19**, 210–225, <https://doi.org/10.1175/JCLI3619.1>.
- Zhang, J., and Coauthors, 2016: The Beaufort Gyre intensification and stabilization: A model–observation synthesis. *J. Geophys. Res. Oceans*, **121**, 7933–7952, <https://doi.org/10.1002/2016JC012196>.
- , W. Weijer, M. Steele, W. Cheng, T. Verma, and M. Veneziani, 2021: Labrador Sea freshening linked to Beaufort Gyre freshwater release. *Nat. Commun.*, **12**, 1229, <https://doi.org/10.1038/s41467-021-21470-3>.
- Zhang, X., M. Ikeda, and J. E. Walsh, 2003: Arctic sea ice and freshwater changes driven by the atmospheric leading mode in a coupled sea ice–ocean model. *J. Climate*, **16**, 2159–2177, <https://doi.org/10.1175/2758.1>.